



White Rose Consortium ePrints Repository

<http://eprints.whiterose.ac.uk/>

This is an author produced version of a paper published in **Engineering Geology**.

White Rose Repository URL for this paper:
<http://eprints.whiterose.ac.uk/archive/1330/>

Published paper

Cousens, T.W. and Stewart, D.I. (2003) *Behaviour of a trial embankment on hydraulically placed pfa*. *Engineering Geology*, 70 (3-4). pp. 293-303.

Behaviour of a Trial Embankment on Hydraulically Placed PFA.

T W Cousens and D I Stewart

School of Civil Engineering

University of Leeds

Leeds, LS2 9JT, UK

ABSTRACT

The paper describes the performance of a 5.3m trial embankment constructed on approximately 45m of hydraulically placed pulverised fuel ash (pfa). It is planned to redevelop the 17 hectare lagoon containing the pfa as a landfill. There is little variation in the particle size distribution of the uniformly graded silt sized pfa over the lagoon. However, the density of the pfa varies with depth with loose material underlying a denser surface layer, in a pattern that probably results from the water level in the lagoon during pfa deposition.

Settlement under the trial embankment was apparently largely complete by the end of the construction period (17 days), with approximately 300mm of settlement under the crest of the embankment. The embankment settlement is significantly affected by compression of the loose layers within the deposit. Analysis of the problem using the conventional one-dimensional settlement method, and an m_v profile determined by CPT calibrated against laboratory tests gave a reasonable prediction of the embankment crest settlement.

Keywords: Case history, embankments, field instrumentation, full-scale tests, industrial wastes, monitoring, settlements, silts.

INTRODUCTION

Much of the electricity generation in the United Kingdom is currently, and has been historically, produced by the combustion of coal. A by product of the process are fine ashes collected by electrostatic precipitation from the flue gases (known as pulverised fuel ashes or pfa) and coarser furnace bottom ashes. Some pfa is used as a cement replacement but a large percentage is disposed of by producing a water-based slurry and pumping it into lagoons where settlement occurs. The result is a site that may have a considerable depth of potentially loose, fine-grained material. These areas have potential for development but there are difficulties constructing on the hydraulically deposited pfa.

This paper describes the construction and performance of a trial embankment on a considerable depth of hydraulically placed pfa. The trial embankment was constructed and monitored to provide large-scale settlement data on the behaviour of the pfa. The site is being developed as a landfill site and the trial was part of a programme to predict the settlement of the underlying pfa in order that basal drainage systems could be designed appropriately.

THE SITE

The site consists of two lagoons which were used for the disposal of pfa from an adjacent coal fired power station. Until about 1948 the area was agricultural, although there are records of coal mining in the area. Opencast coal mining and the extraction of sand and gravel during the 1950s and 60s resulted in large voids. These were partially backfilled with colliery spoil

and embankments of the same material were constructed to form lagoons for the disposal of pfa. The pfa was pumped into the lagoons as a water slurry. The pfa was allowed to sediment and excess water was decanted off and disposed of into a nearby river. Pfa disposal took place from 1970 to 1994.

The trial embankment reported in this paper was constructed towards the middle of the larger lagoon on the site (17 hectares in extent). A plan of the lagoon and embankment is shown in Figure 1. Slurry inputs into this lagoon appear to have been largely to its NW corner.

SITE INVESTIGATION

Several site investigations have been conducted at the site, but, as part of the study reported here, additional investigations were performed to determine the extent of the pfa and its characteristics. Cone penetrometer (CPT) and pressuremeter testing was carried out at various locations in the lagoon to determine the in-situ behaviour and variability of the pfa. Disturbed and undisturbed samples were collected from five boreholes located around the lagoon both to characterise the pfa and to investigate its spatial variation. Figure 1 shows the locations of the various in-situ tests and boreholes. Laboratory tests included particle size distributions, liquid and plastic limits and one-dimensional compression tests.

At the location of the trial embankment the surface of the pfa is at approximately 25m AOD with a slight fall from north to south. The maximum depth of pfa is about 45m with the ground water level 6m below ground level. The minimum depth of pfa within 40m horizontal distance of the trial embankment is about 20m.

Figures 2 shows CPT data from a location near to the trial embankment as indicated on Figure 1. The data is typical of that obtained from the CPT tests and shows variations in the response of the pfa which is described as varying from firm to very loose. The CPT data also showed the depth of the pfa. Figures 3a and 3b are plots of the relative density of the pfa against depth determined using CPT data from two locations close to the trial embankment. These values were produced using the method described by Meigh (1987), and are based on the cone resistance values and the in-situ vertical stress. Figure 3 is primarily intended to show patterns in the relative density of the pfa, and the absolute values should be treated with caution. The relative density plot shows an upper denser layer overlying a very loose central layer, above denser material. Other CPTs conducted in the vicinity of the embankment showed a similar pattern for the pfa.

DESCRIPTION OF THE PFA

Figure 4 shows the particle size distribution of a sample taken from a depth of 14.5m in borehole 1B (i.e. near the embankment location). The particle size distributions of most of the samples taken from the site were very similar, and suggest that the pfa is relatively uniform over the site with 5-10% clay sized particles and 60-80% silt sized. This is fairly typical for pfa, which tend to be predominantly silt sized (Cabrera et al., 1984; McLaren and DiGioia, 1987). Occasional thin coarse layers were detected in the pfa, but their extent is unknown although they appear to be limited.

The average liquid limit of the pfa was 46% (range 38-56%) with an average plastic limit of 42% (range 32-54%). The average plasticity index was 4% with some samples showing no plasticity. The pfa classifies as an inorganic silt with slight plasticity. The in-situ moisture content of the pfa showed a general pattern of a central band with a very high moisture

content (55% to 78%) with lower values above and below (38% to 44%). These values suggest loose material, especially in the central band. The in-situ bulk density is estimated as varying between 1.54 and 1.66 Mg/m³, which correspond to void ratios of 1.1 to 1.6, the latter values corresponding with the soft zone. This voids ratio is quite high; for example, in the extended Casagrande soil classification system void ratio values for silt at maximum dry density at optimum compaction are given as less than 0.7 (Road Research Laboratory, 1952).

Figure 5 shows the coefficient of volume compressibility measured in one-dimensional compression tests on notionally undisturbed specimens taken from U100 samples recovered from the boreholes. Recovery of U100 samples from the pfa was extremely difficult in the very loose layer, and it is likely that these had suffered significant disturbance probably resulting in densification. Thus the compressibility of the loose layer may have been underestimated. All the one-dimensional compression specimens were saturated before testing, as the primary aim was to investigate the suitability of the site for a landfill, and this condition represents the worse case design scenario for the water table under the basal liner. Therefore the compressibility data for specimens taken from above the water table (19m AOD) will over-estimate the compressibility under field conditions if the pfa above the water table is stabilised by capillary water suction in-situ.

The coefficient of volume compressibility can also be estimated from CPT data using the equation:

$$m_v = 1/(\alpha \cdot q_c) \quad (1)$$

where q_c is the cone resistance and α is a constant of proportionality that depends on the soil type (Meigh, 1987). Meigh suggests that α is in the range 3 to 11 for normally consolidated sands and 3 to 6 for low to medium plasticity silts. The CPT data from locations 4 and 6

situated close to the trial embankment have been used to estimate the compressibility of the pfa (CPT 5 was not used due to its proximity to the lagoon edge). The data was fitted by (i) initially assuming an arbitrary value of α to produce m_v profiles for comparative purposes, (ii) determining the trend in each CPT compressibility profile by eye, (iii) estimating a composite average compressibility profile, and (iv) fitting this composite compressibility profile to the one-dimensional compression data for depths below 0m AOD by selecting the appropriate α value. The variation in the coefficient of volume compressibility with depth determined in this way (where $\alpha=11$) is shown as a solid line in Figure 5. It is estimated that the coefficient of volume compressibility, m_v , was approximately $0.08\text{m}^2/\text{MN}$ to a depth of about 10m below ground level, reached a maximum of about $0.18\text{m}^2/\text{MN}$ in the loose layer, and decreased to a fairly steady value of $0.04 \text{ m}^2/\text{MN}$ at depths greater than about 32m below ground level. The pattern in the variation of m_v with depth is a clear trend in the data from each CPT. These values of m_v indicate that the pfa has a compressibility comparable to stiff clays (Tomlinson, 1995). Figure 6 compares the idealised compressibility profile with the data from CPTs 4 and 6. While there is variation in the m_v profiles between the locations, the assumed profile is a good fit to the main trends in the CPT data.

TRIAL EMBANKMENT AND INSTRUMENTATION

The trial embankment had a crest area of about 10 by 50m, a base area of 37 by 71m and a final constructed height of 5.3m. The dimensions of the embankment were chosen so that deformations at the centre section could be considered as approximating to plane strain conditions. The side slopes were about 22° to give reasonably slow changes in the imposed loading on the underlying pfa and ensure stable sides to the embankment. The embankment was constructed on a geogrid overlain with a woven geotextile placed directly onto the pfa (which was cleared of vegetation). The embankment consisted of approximately 0.25m of

crushed stone separated by a woven geotextile from 0.5m of colliery spoil, 4m of pfa and 0.5m of colliery spoil. Over the central portion of the embankment a bentonite-impregnated geotextile was placed on the lower layer of spoil. The bottom 0.75m of the central portion of the embankment was representative of the landfill liner that is proposed for the site, and the surface layer of colliery spoil was placed to protect the pfa from erosion by wind and rain.

Instrumentation was installed on two planes through the embankment. Both instrumented planes were at right angles to the long axis of the embankment, one at the centre of the embankment with a secondary section five meters away and parallel to it, to act as a back-up in case of damage to the main section (see Figures 7 and 8). The instrumentation comprised inclinometers, magnetic settlement gauges (the gauge positions are not shown in figures 7 and 8 because the deepest gauge is approximately 30m below ground level), hydraulic profile gauges and standpipe piezometers. An array of pneumatic piezometers were also installed but gave erratic readings. The elevations of the embankment crest, and of selected points around the embankment, were monitored using a surveying total station. Most of the data reported in this paper are from the magnetic settlement gauges and the surface monitoring points.

CONSTRUCTION SEQUENCE

The instrumentation was installed shortly before the construction of the embankment due to time constraints. After installation all the instrumentation was tested. Construction of the embankment commenced around the 10th September, 1999, (day 4 on Figure 9) and took fourteen days to complete. Construction used pfa from the second lagoon and colliery spoil from an embankment. There was one period of heavy rain during construction (day 14). At one stage a large vibrating roller was used but resulted in marked ground vibrations and was abandoned.

PERFORMANCE OF THE EMBANKMENT

Figure 9a shows the average height of the embankment with time. After completion of the embankment the reported data are averaged from ten points on the crest of the embankment.

Figure 9b shows average crest settlement after the embankment was complete (i.e. day 18 onwards). Figure 9b indicates that from about day 20, shortly after the embankment was complete, there was no significant settlement of the crest. An additional reading at 150 days confirmed this pattern. The accuracy of individual readings was estimated as +/- 10mm.

Figures 10 and 11 present the magnetic settlement gauge data for gauges 2 and 3 (located at the base of the shoulder and at the midpoint of the embankment respectively). Gauge 1 was damaged during construction of the embankment. The accuracy of the reported elevations is estimated as being +/- 5mm. The data presented in Figure 10 has been corrected for two aberrant events that occurred between days 17 and 18 and between days 21 and 23. In both cases the event consisted of an apparent uniform heave of all the magnets in gauge 2 (the deepest is 30m below original ground level). It is extremely unlikely that such a heave could have resulted from actual soil movements, and may indicate that buckling of the tube occurred. It was noted at about this time that it became more difficult to lower the probe down the tube. This uniform heave has been deducted from the data (indicated by the break in the line). For gauge 3 the settlements of only the two near surface magnets are reported because buckling of the tube prevented access to the deeper magnets.

Figures 10 and 11 indicate that significant settlement of the near surface pfa occurred during embankment construction, with approximately 0.3m of settlement occurring at the gauge 1.6m below the centre of the embankment. The settlement at 1.2m under the shoulder of the

embankment was approximately 0.12m. After that time there was a slight settlement of all monitoring points over the next ten days after which the points were essentially stationary.

Figure 12 shows the settlement profile across the embankment in the plane of the main instrumentation array, measured by a hydraulic settlement profile gauge. The profile tube was situated approximately 1m below original ground level. The settlement increased steadily from a very small value under the toe of the embankment slope to a maximum value under the full height of the embankment. There is good agreement between the magnetic settlement gauge and the hydraulic settlement profile gauge data, with a measured long-term settlement using the profile gauge of about 0.1m under the embankment shoulder close to the location of magnetic settlement gauge 2 and 0.3m under the centre of the embankment.

The inclinometer data (not shown) showed only very small lateral movements. These were less than 10mm below 1.5m below original ground level, and less than 50mm above this where it is thought that the installations may have been affected by plant movement and the placing of fill.

ANALYSIS

The settlements of the embankment have been analysed using the one-dimensional method of Terzaghi (1943), where the vertical stress increase is calculated using isotropic elasticity, and the strains are assumed to be one-dimensional and are calculated from the coefficient of volume compressibility, m_v . In the analysis m_v was assumed to vary only vertically, and was estimated from the composite average profile plotted as a solid line in Figure 5. The vertical stress increase under the central cross-section has been calculated on the assumption that the

embankment is long in comparison with its height using the solution to the elastic equations for embankment loading presented by Das (1990).

The continuous solid line in Figure 12 is the settlement profile calculated using the method above which can be compared with that measured at the primary instrumented cross-section by the hydraulic settlement gauge. While the shapes of the two profiles are broadly similar, and the measured and predicted settlements beneath the edge of the embankment are about the same, the maximum measured settlement (beneath the centre-line of the embankment) exceeds the predicted value by about 20% (approximately 300mm compared with 240mm).

In the analysis it has been assumed that, for a particular soil type, compressibility can be determined from CPT data using equation 1 (where $m_v \propto 1/q_c$), and for comparative purposes the settlement analysis has been repeated to determine the constant of proportionality ($1/\alpha$) compatible with the measured maximum settlement. The dashed line in Figure 12 is the result of this exercise and gives $\alpha=9$. However, although the predicted settlement beneath the centreline of the embankment is correct, that beneath and beyond the edges of the embankment is now overestimated.

DISCUSSION

The pattern of movements under the trial embankment is complex with a vertical movement of about 300mm beneath the central section. The movement appears to have ceased shortly after the completion of the construction of the embankment when the maximum increase in vertical effective stress is about 89kPa. The crest of the embankment did not move significantly over 130 days following completion. The overall pattern of surface settlement,

observed using the hydraulic profile gauges, was similar to that reported in standard texts (Road Research Laboratory, 1952).

The CPT data suggests that there is a denser surface layer of pfa about 8 to 10m thick (lower level 17 to 15m AOD) overlying very loose pfa. The loose layer is of variable thickness, although the composite average CPT data in Figure 5 indicates the typical thickness. This may be the result of the depositional history of the pfa and the effect of changing water levels. The water table is currently about 6m below the surface of the pfa (about 19m AOD). The river into which the site drains is about 14.2m AOD as it passes the site. When the slurried pfa was pumped into the lagoon, it is likely that the original open cast void would have filled with water to a level above 14.2m AOD before the excess water from the slurry could overflow into the river. Thus the pfa below about 15m AOD may have settled through water, whereas the pfa above this level probably settled from the slurry as it braided across the surface of the pfa. The upper layers have probably also been subjected to cycles of wetting and drying, which would have tended to consolidate them.

Data from the magnetic settlement gauges can be used to estimate average vertical strains in the zones between the individual magnets. Data from settlement gauge 2 (under the shoulder of the embankment) indicates that at the end of the monitoring period, when settlement had effectively ceased, the vertical strain in the region between 1.2 and 7.6m (23.9 and 17.5 AOD) was about 0.7%. At depths between 7.6 and 13m (17.5 and 12.1 AOD) the vertical strain was approximately 1%, between 13m and 29.4m it was about 0.2% and below 29.4m there is essentially no movement. Data from magnetic settlement gauge 3 (below the centre of the embankment) indicates that the vertical strain at depths between 1.6m and 4.4m below original ground level (approximately 23.5m and 20.7m AOD) was about 1%. At some point

below this depth (between about 4 and 8m) the tube of settlement gauge 3 buckled, which may have resulted from the tube passing through a zone of large vertical strains.

Using an α value of 11 the analysis predicts that at the location of settlement gauge 2 the vertical strain was about 0.2% to a depth of 10m, was about 0.5% between 10 and 24m below original ground level, and averaged about 0.1% from 24m to the bottom of the pfa. Under the embankment centreline (the location of settlement gauge 3), the vertical strain in the top five metres was about 0.7%, with strains of about 1.1% between 13 and 16m below original ground level. Thus the analysis using an α value of 11 predicts vertical strains under the centre of the embankment that are approximately 70% of the measured values (which correlates well with the prediction of overall settlement). However, under the edge of the embankment, it significantly under-predicts vertical strains at shallow depths, but predicts vertical strains to a greater depth than observed. It does, however, indicate the influence of the soft layer.

Differences in both the magnitude of displacements and the pattern of vertical strains predicted by the analysis from those observed may partly be caused by (a) assuming one-dimensional compression of the pfa, (b) the accuracy of the predicted vertical stress increases, and (c) the accuracy of the compressibility values assumed for the pfa. The inclinometer data indicate that deformation was essentially one-dimensional, and thus the use of Terzaghi's one-dimensional method would appear to be appropriate. The error in vertical stress increase caused by assuming isotropic elasticity is about $\pm 20\%$ even when the soil is systematically non-homogeneous, anisotropic and non-linear (Padfield and Sharrock, 1983). However it is known that elastic analyses tend to give a wider dispersion of vertical stress increases than occurs in soils deforming plastically, which may partly explain the difference between the

predicted and measured strain patterns (particularly the depth to which strains are predicted below the edge of the embankment).

It would appear that the use of laboratory tests and CPT data to produce a profile of m_v with depth generally underestimates the m_v values, if it is assumed that under the centre of the embankment the analysis should produce a reasonable estimate of the increases in vertical effective stress. However the underestimate may not be constant, as the use of a single α value for a deposit of widely varying density may not be appropriate, and indeed common usage tends to correlate α to density. Also, the laboratory m_v values were calculated based on a 100kPa stress increase. This is an appropriate range for the zone of pfa immediately below the embankment crest, but further away the stress increase is much lower, and so the m_v values found using a 100 kPa increment may be inappropriate. For example, m_v will be under-estimated if the stress increase in-situ is less than 100kPa where the pfa is normally consolidated. This effect may explain why strain magnitudes are less well predicted below the edge of the embankment. Another factor not considered in the analysis is that vibration and disturbance during construction (resulting from heavy construction plant movements) may have caused additional settlement, especially in the softer zone.

Despite the reservations discussed above, the use of a compressibility profile based on CPT data calibrated using laboratory values of m_v , together with expected stress increases derived using elastic theory appears to give a reasonable prediction of settlement beneath the central axis of a symmetrically loaded area.

CONCLUSIONS

The hydraulically placed pfa, which is a uniformly graded silt sized material, shows significant variations in relative density. These variations are primarily thought to reflect the water level in the lagoon during deposition. Specifically, it is suggested that the pfa that settled through water is looser than the pfa that settled out of water flowing across an exposed pfa surface.

The trial embankment that was constructed on this deep deposit of uniformly graded silt sized pfa reached full settlement shortly after the end of the construction. The shape of the settlement profiles suggests that variation in pfa compressibility in lateral directions had little effect. The settlement appeared to be significantly affected by compression of loose layers within the deposit.

Sampling of very loose zones in the pfa was very difficult, if not impossible using standard techniques. Analysis of the problem, using the conventional one-dimensional settlement method, suggests that with sampling and conventional laboratory testing to calibrate the data, CPT data may be useful. In this case an α value (the constant of proportionality between constrained modulus and the cone resistance) of 11 gave a reasonable fit to field settlement data beneath the crest of the embankment, and a value of 9 provided a good fit. However a constant α value may not be appropriate for deposits of such variable density.

ACKNOWLEDGEMENTS

The authors would like to thank Mr John Ablitt and Biffa Waste Services Ltd. for permission to use the information and data used in this paper.

REFERENCES

- Cabrera, J G, Braim, M and Rawcliffe, J. (1984). The use of pulverised fuel ash for structural fills. Second Int. Conf on Ash Technology and Marketing, London, pp529-533.
- Das, B.M. (1990). Principles of Foundation Engineering. 2nd Edition. PWS-Kent.
- McLaren, R J and DiGioia, A M. (1987). The typical engineering properties of fly ash. Geotechnical Special Publication No 13. ASCE, pp683-697.
- Meigh, A.C. (1987). Cone penetration testing- methods and interpretation. CIRIA- Butterworths.
- Padfield, C.J. and Sharrock, M.J. (1983). Settlement of Structures on Clay Soils. CIRIA Special Publication 27, Construction Industry Research and Information Association.
- Road Research Laboratory (1952). Soil Mechanics for Road Engineers. HMSO, London.
- Somers, N R. (2000). Secondary lines at Gale Common ash disposal scheme. Ground Engineering, 33, No.8, pp30-34.
- Terzaghi, K. (1943). Theoretical Soil Mechanics. John Wiley.
- Tomlinson, M J. (1995), Foundation Design and Construction. Longman Scientific and Technical, UK.

Figures

Figure 1. Plan of the pfa lagoon showing the position of the trial embankment and the location of the site investigation

Figure 2. CPT data from location C4 (close to the trial embankment)

Figure 3. (a) Relative density profile determined from CPT4, and (b) Relative density profile determined from CPT6

Figure 4. Particle size distribution for the pfa.

Figure 5. Coefficient of volume compressibility measured in the laboratory and by CPT

Figure 6. Comparison between the assumed volume compressibility profile (solid line) and m_v data (assuming $\alpha=11$) from (a) CPT4 and (b) CPT6.

Figure 7. Schematic of the primary instrumented embankment cross-section.

Figure 8. Schematic of the secondary instrumented embankment cross-section.

Figure 9. Variation in embankment height and crest settlement with time.

Figure 10. Settlements beneath the shoulder of the embankment (magnetic settlement gauge 2)

Figure 11. Settlements beneath the crest of the embankment (magnetic settlement gauge 3)

Figure 12. Settlement profile in the plane of the main instrumentation array (HG1, day 27)

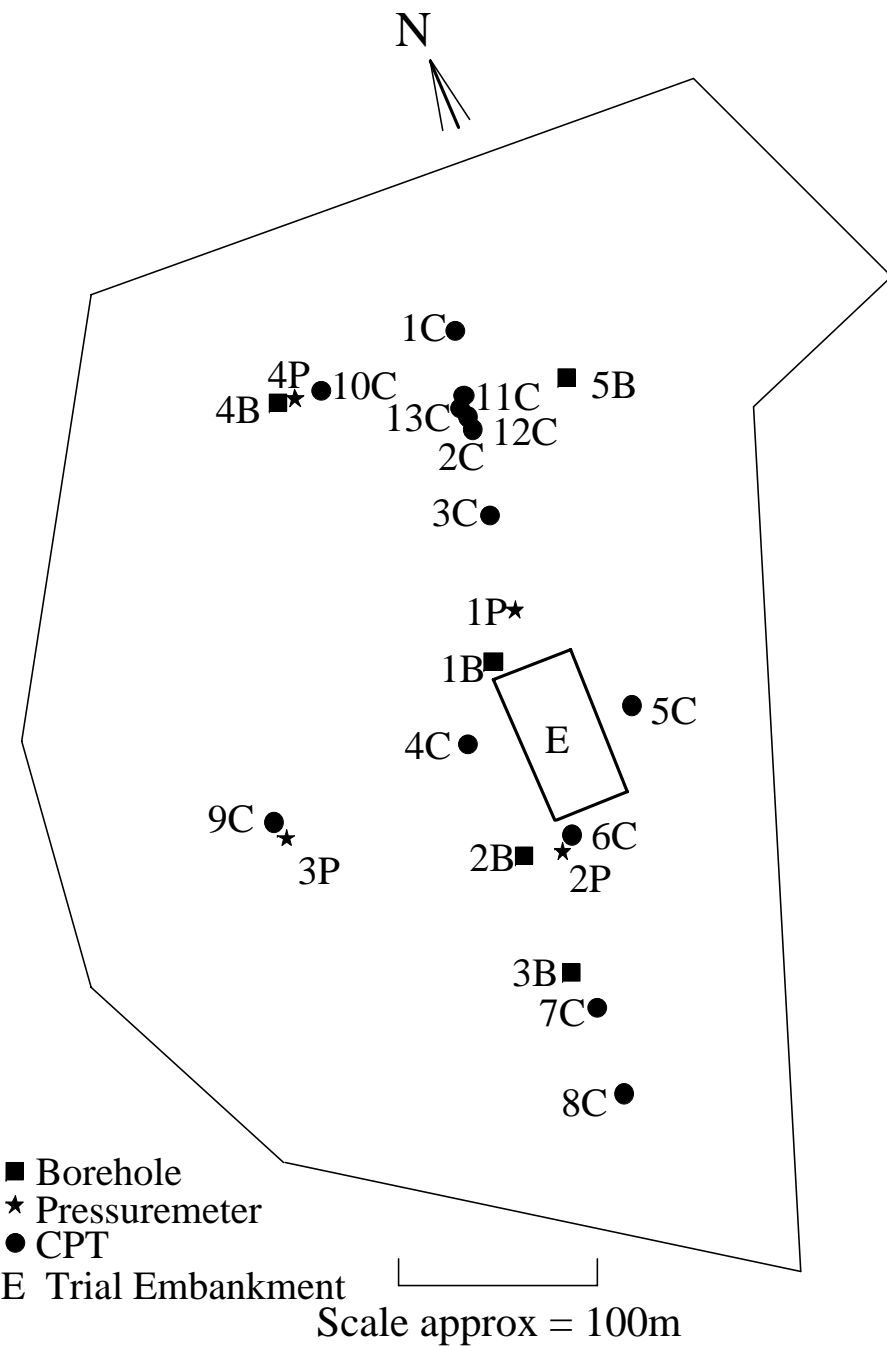


Figure 1. Plan of the pfa lagoon showing the position of the trial embankment and the location of the site investigation

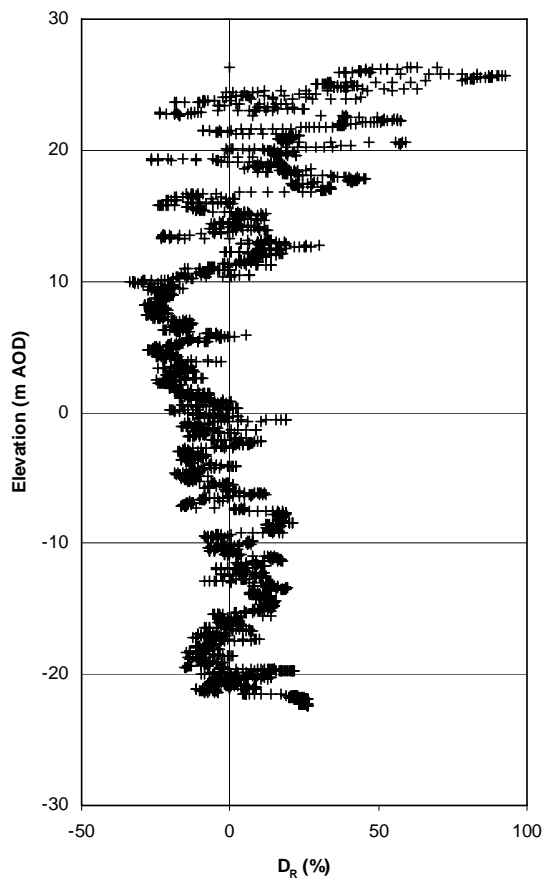


Figure 3a. Relative density profile determined from CPT4

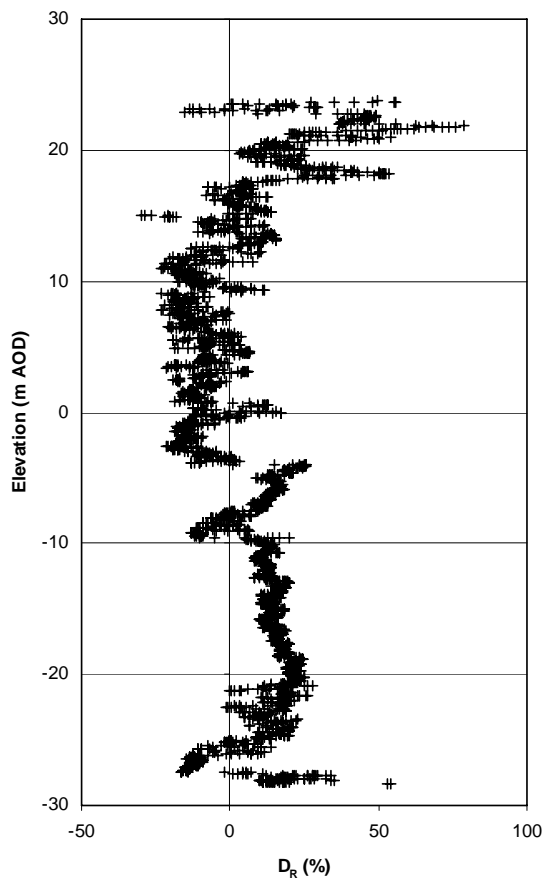


Figure 3b. Relative density profile determined from CPT6

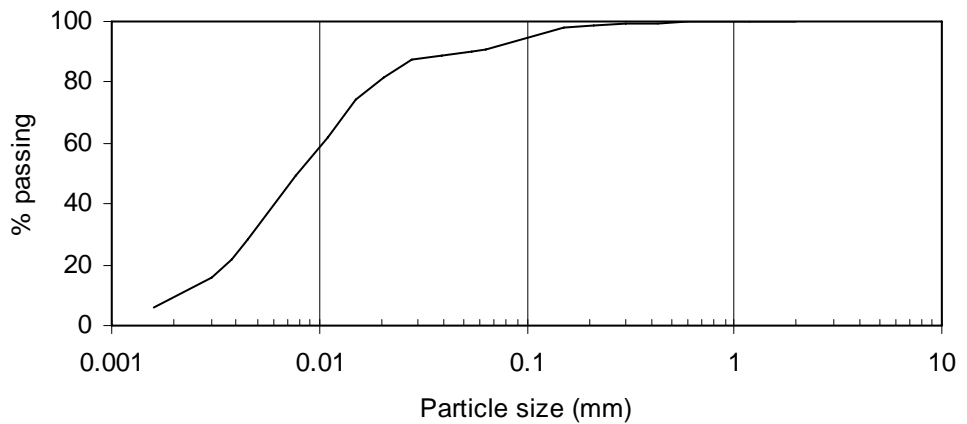


Figure 4. Particle size distribution for the pfa.

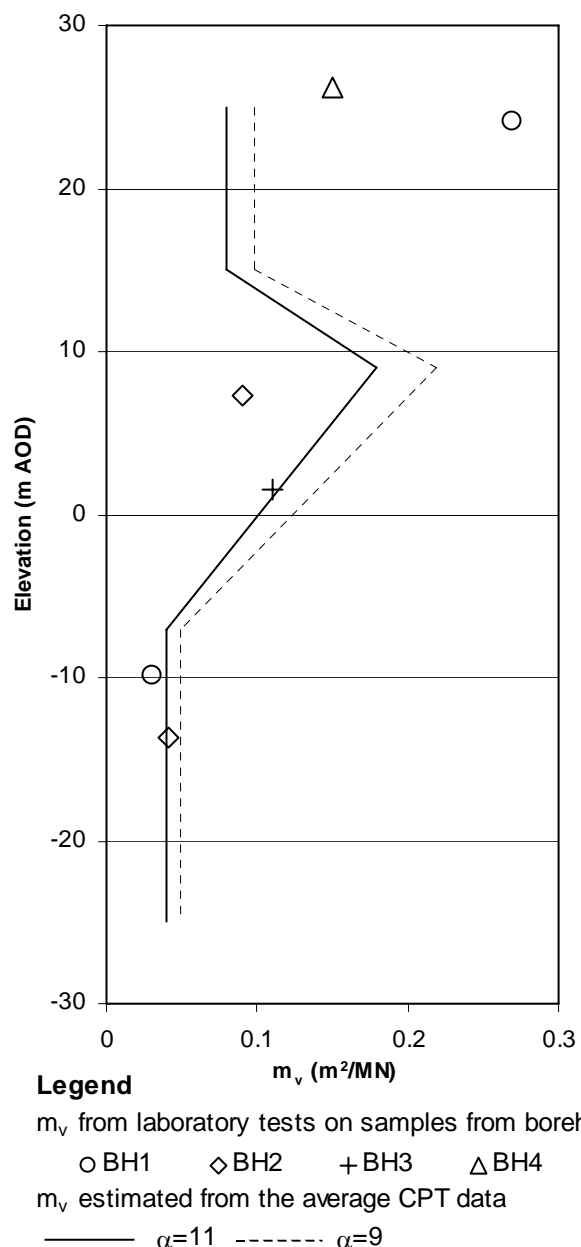


Figure 5. Coefficient of volume compressibility measured in the laboratory and by CPT

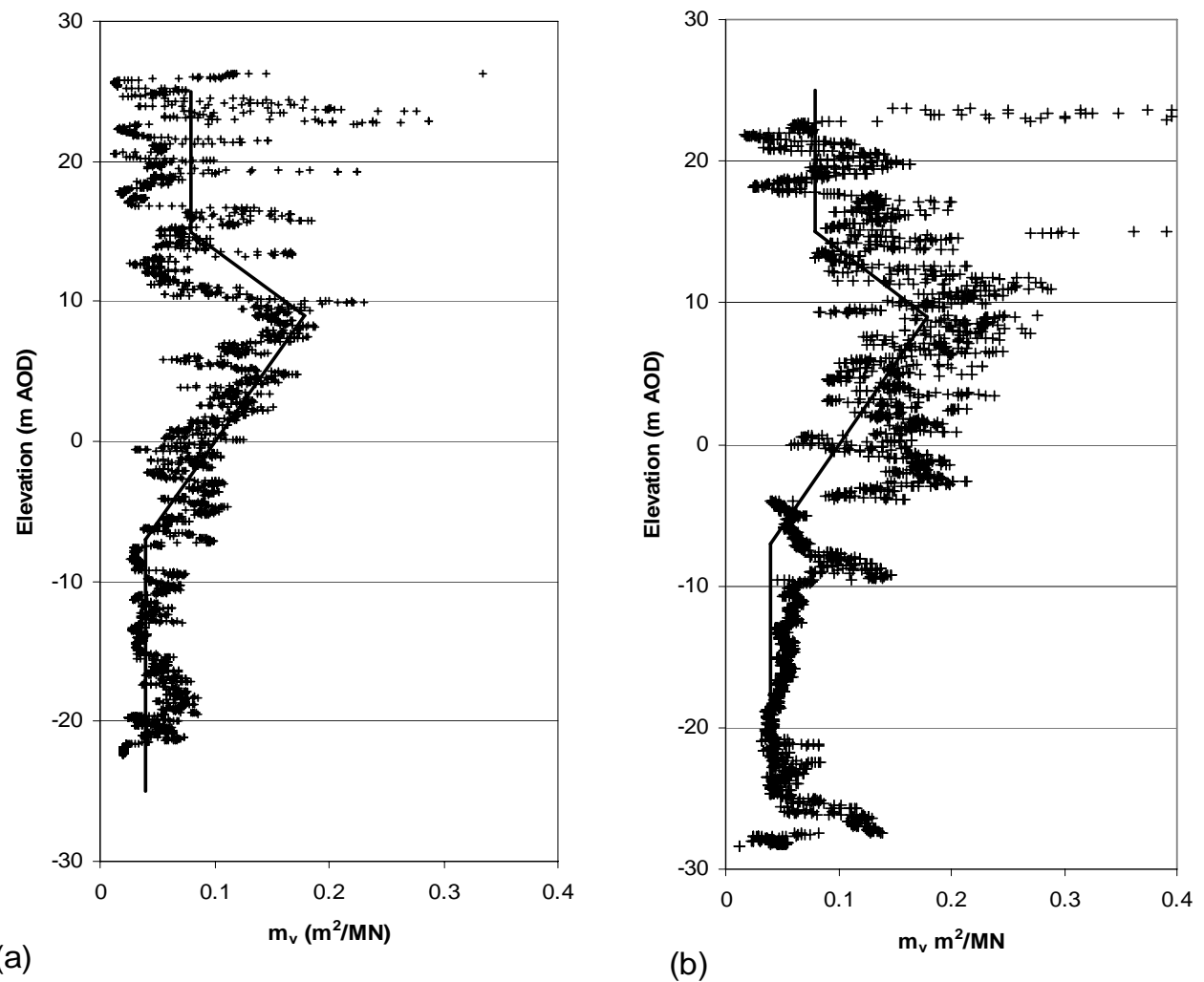


Figure 6. Comparison between the assumed volume compressibility profile (solid line) and m_v data (assuming $\alpha=11$) from (a) CPT4 and (b) CPT6.

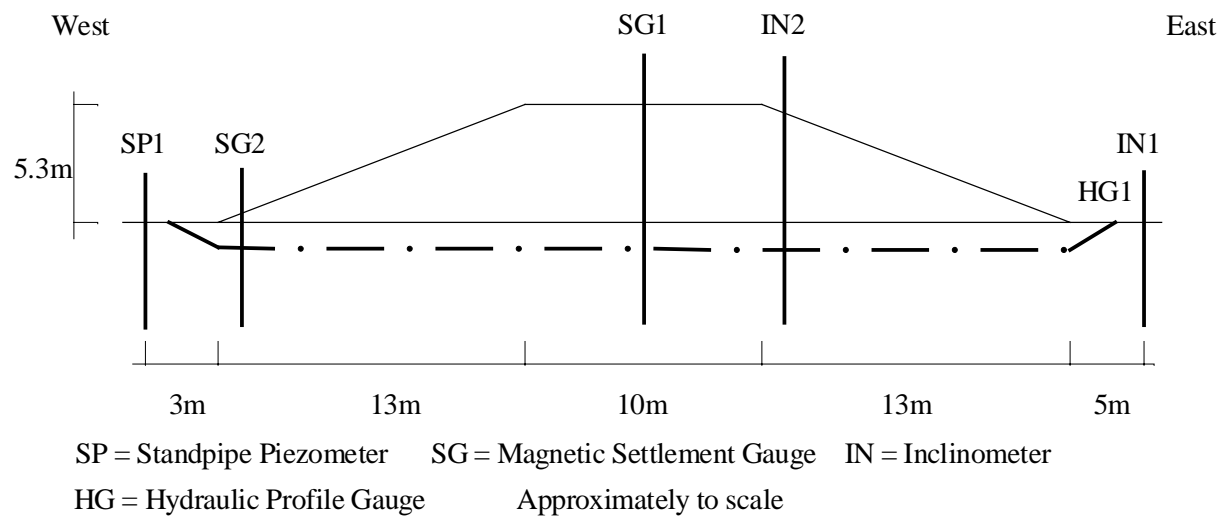


Figure 7. Schematic of the primary instrumented embankment cross-section.

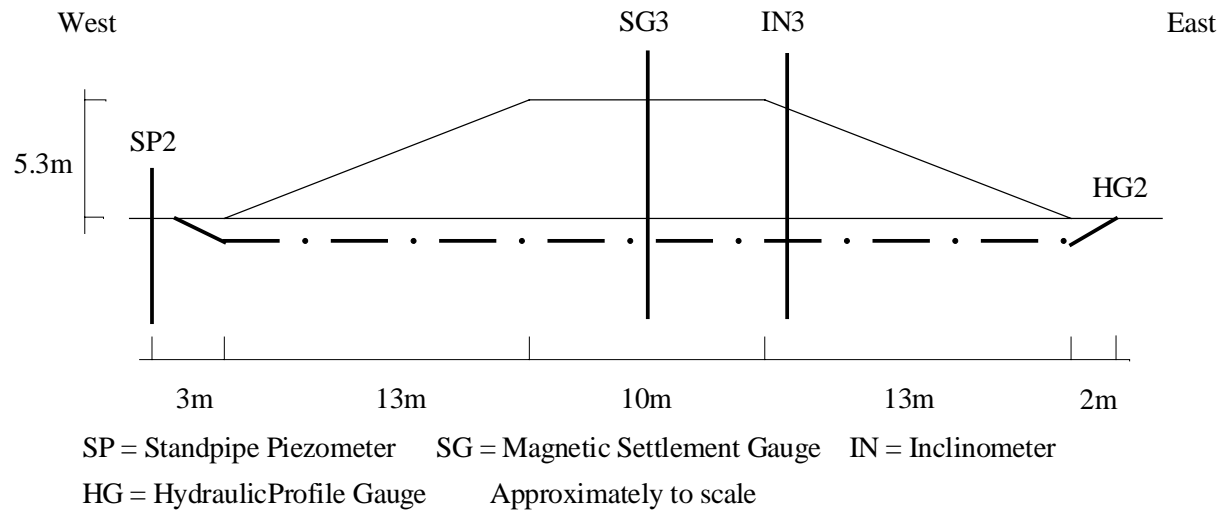


Figure 8. Schematic of the secondary instrumented embankment cross-section.

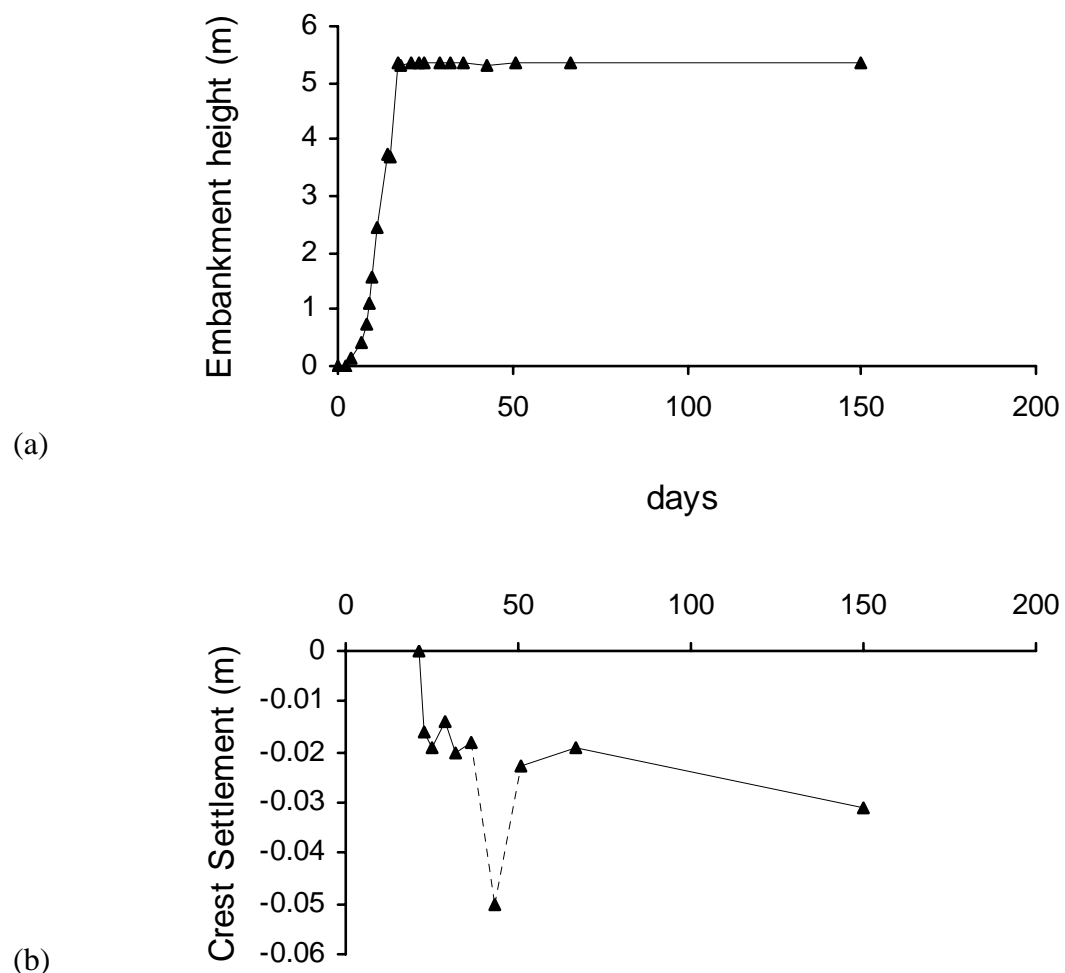


Figure 9. Variation in embankment height and crest settlement with time.

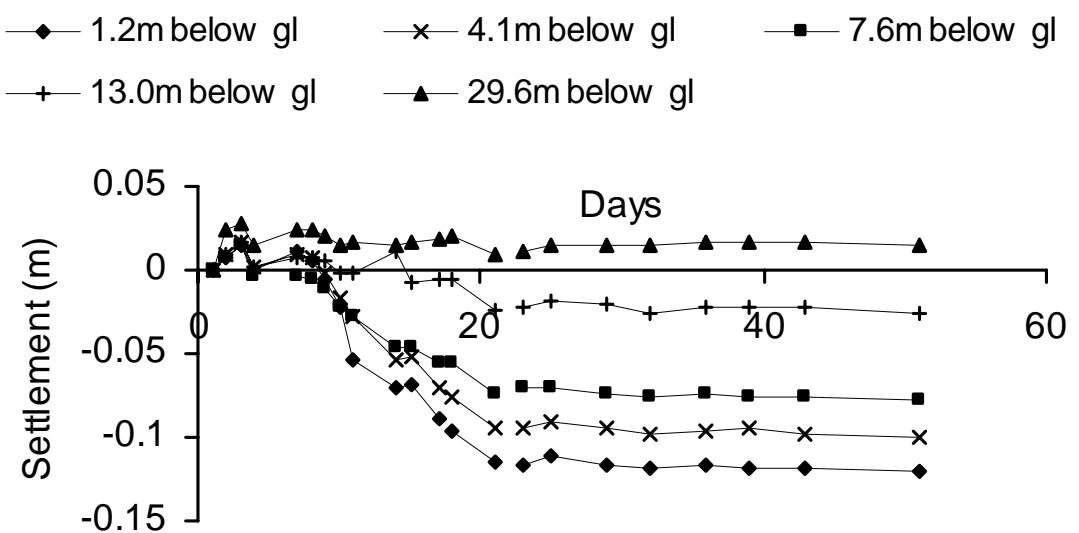


Figure 10. Settlements beneath the shoulder of the embankment (magnetic settlement gauge 2)

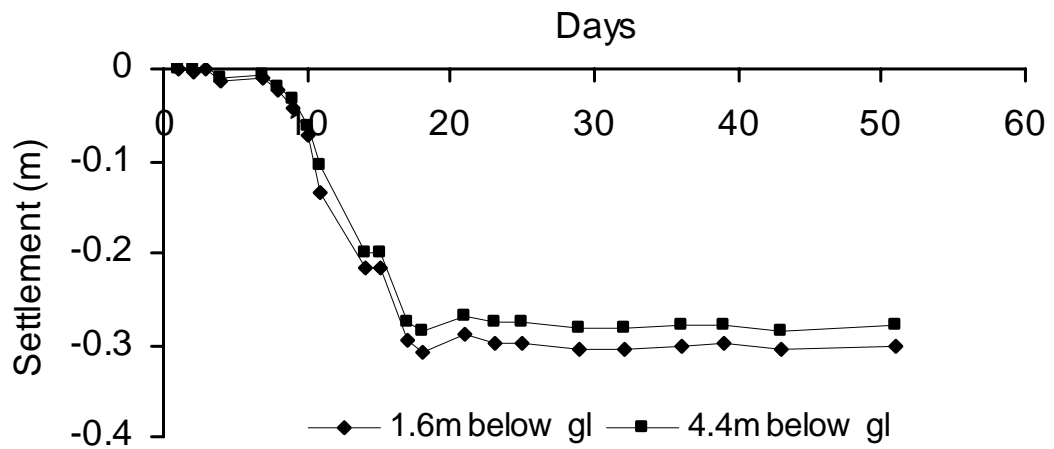


Figure 11. Settlements beneath the crest of the embankment (magnetic settlement gauge 3)

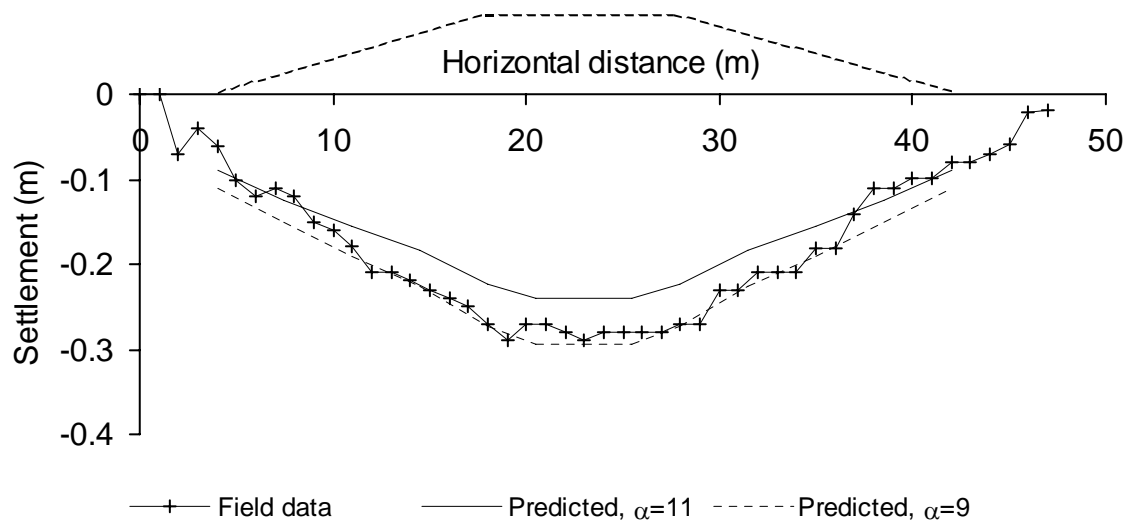


Figure 12. Settlement profile in the plane of the main instrumentation array (HG1, day 27)